

Supplementary Materials: The Vip3Ag4 Insecticidal Protoxin from *Bacillus thuringiensis* Adopts A Tetrameric Configuration That Is Maintained on Proteolysis

Leopoldo Palma, David J. Scott, Gemma Harris, Salah-Ud Din, Thomas L. Williams, Oliver J. Roberts, Mark T. Young, Primitivo Caballero and Colin Berry

| | | | | | |
|-------------------|-------------------|-------------------|-------------------|-------------------|-------------------|
| MGSSHHHHHH | SSGLVPRGSH | MASMTGGQQM | GRDPMNKNNT | KLNARALPSF | IDYFNGIYGF |
| 36 | 46 | 56 | 66 | 76 | 86 |
| ATGIKDIMNM | IFKTDTGGNL | TLDEILKNQQ | LLNEISGKLD | GVNGSLNDLI | AQGNLNTELS |
| 96 | 106 | 116 | 126 | 136 | 146 |
| KEILKIANEQ | NQVLNDVNNK | LNAINTMLHI | YLPKITSMLN | DVMKQNYALS | LQIEYLSKQL |
| 156 | 166 | 176 | //186 | 196 | // 206 |
| QEISDKLDVI | NVNVLINSTL | TEITPAYQRM | KYVNEKFEDL | TFATETTLKV | KKNSSPADIL |
| 216 | 226 | 236 | 246 | 256 | 266 |
| DELTELTELA | KSVTKNDVDG | FEFYLNTFHD | VMVGNNLFGR | SALKTASELI | AKENVKTSGS |
| 276 | 286 | 296 | 306 | 316 | 326 |
| EVGNVYNFLI | VLTALQAKAF | LTLLTCRKLL | GLADIDYTFI | MNEHLDKEKE | EFRVNILPTL |
| 336 | 346 | 356 | 366 | 376 | 386 |
| SNTFSNPNYA | KAKGSNEDAK | IIVEAKPGYA | LVGFEMSnds | ITVLKAYQAK | LKQDYQVDKD |
| 396 | 406 | 416 | 426 | 436 | 446 |
| SLSEIVYGDM | DKLLCPDQSE | QIYYTNNIAF | PNEYVITKIT | FTKKMNSLRY | EATANFYDSS |
| 456 | 466 | 476 | 486 | 496 | 506 |
| TGDIDLNKTK | VESSEAEYST | LSASTDGVYM | PLGISETFL | TPINGFGIVV | DENSKLVNL |
| 516 | 526 | 536 | 546 | 556 | 566 |
| CKSYLREVLL | ATDLSNKETK | LIVPPIGFIS | NIVENGNLEG | ENLEPWKANN | KNAYVDHTGG |
| 576 | 586 | 596 | 606 | 616 | 626 |
| VNGTKALYVH | KDGEFSQFIG | DKLKSKETYV | IQYIVKGKAS | ILLKDEKNGD | CIYEDTNNGL |
| 636 | 646 | 656 | 666 | 676 | 686 |
| EDFQTITKSF | ITGTDSSGVH | LIFNSQNGDE | AFGENFTISE | IRLSEDLSP | ELINSDAWVG |
| 696 | 706 | 716 | 726 | 736 | 746 |
| SQGTWISGNS | LTINSNVNGT | FRQNLSSLESY | STYSMNFNVN | GFAKVTVRNS | REVLFEKNYP |
| 756 | 766 | 776 | 786 | | |
| QLSPKDISEK | FTTAANNTGL | YVELSRFTSG | GAINFRNFSI | K | |

Figure S1. Sequence of the Vip3Ag4 protein. Bold letters represent the sequence added to the N-terminus from the expression construct and including the His-tag. Trypsin cut sites are shown as // above the two amino acids separated by the cleavage. Numbering is given for the full-length, naturally-occurring Vip3Ag4 sequence.

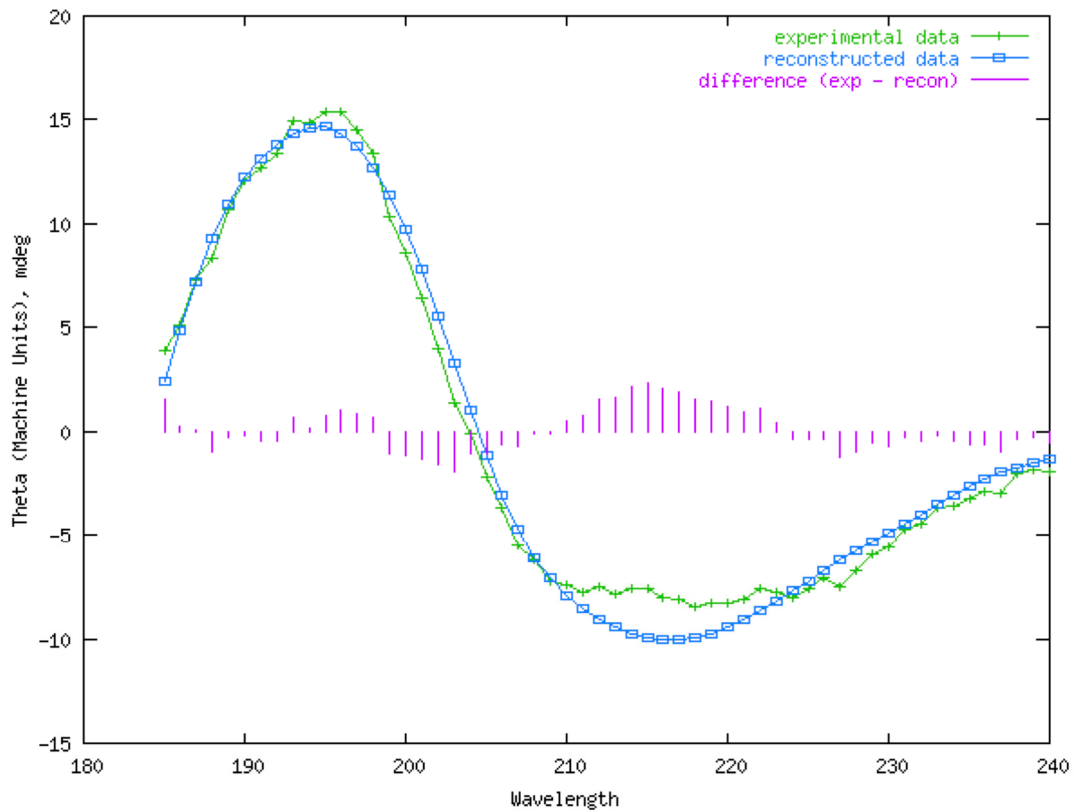


Figure S2. CD analysis of Vip3Ag4. The trace for the 0.25 mg/ml Vip3Ag4 sample is shown between 185 and 240 nm. The green curve represents the experimental data, the blue curve the data generated from the reference set, and the pink lines show the difference between the experimental data and the reference data.

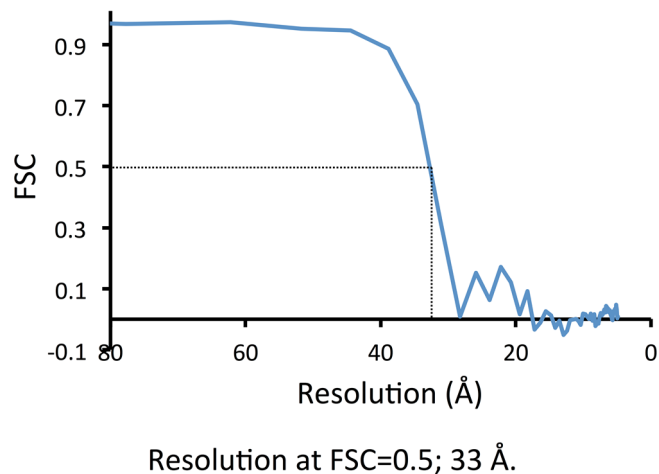


Figure S3. Vip3Ag4 FSC curve. The curve for the 14th iteration of the EMAN model is shown and indicates a resolution of ~33 Å.

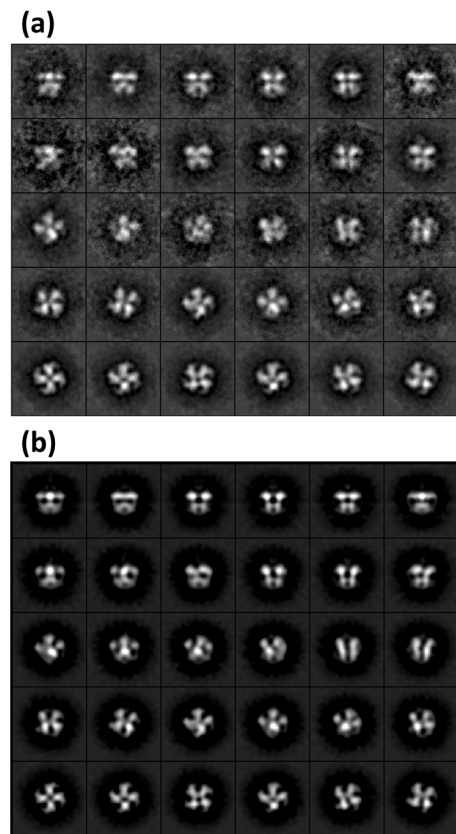


Figure S4. Vip3Ag4 nanogold TEM 2D class averages. (a) 2D-class averages for Vip3Ag4 gold-labelled particles. (b) reprojections from the final 3D model.

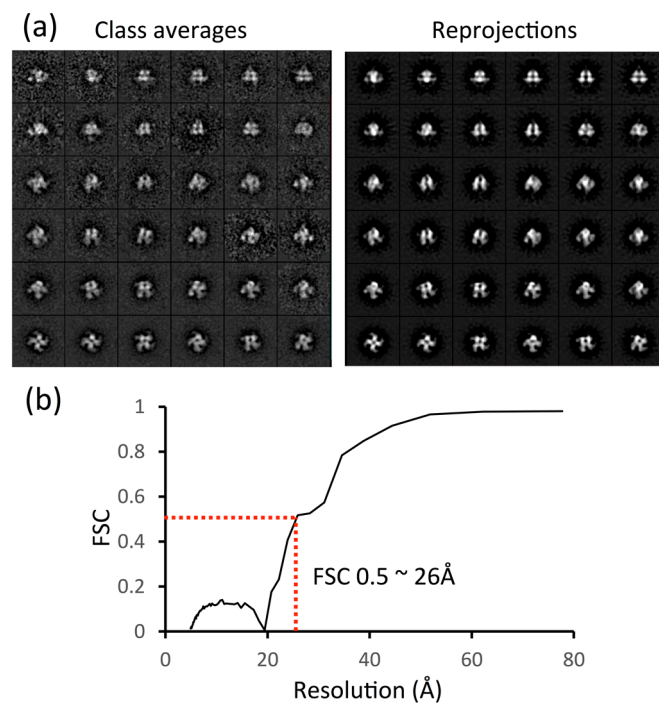


Figure S5. (a) Class averages (left) and 2D-reprojections (right) from the 3D model of trypsin-treated Vip3Ag4. (b) Fourier shell correlation (FSC) of 3D-structures derived from even- and odd-numbered particles indicating a resolution (FSC 0.5 criterion) of approximately 26 Å.

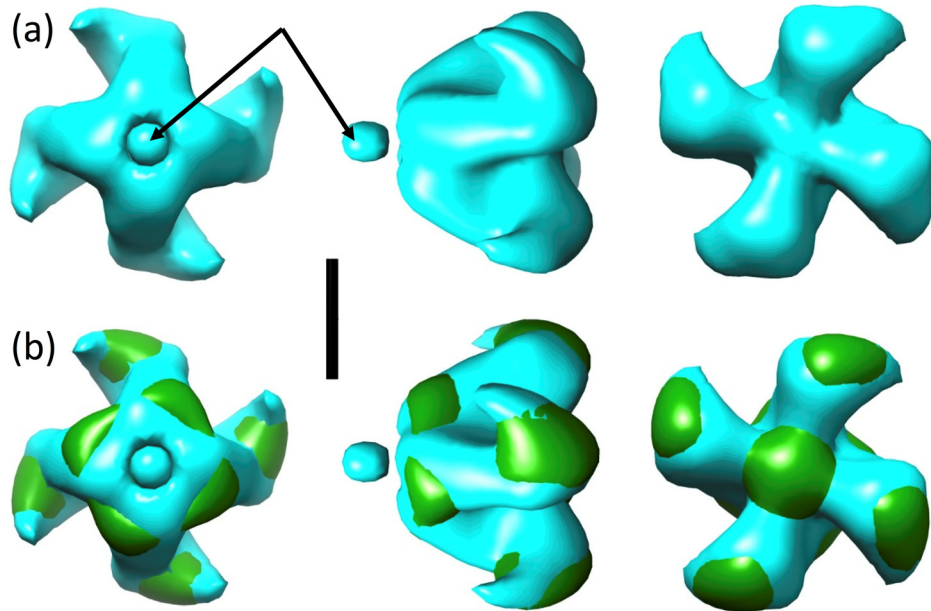


Figure S6. (a) 3 views of 3D-structure of trypsin-treated Vip3Ag4. A small region of disconnected density (likely to have resulted from some mis-classification of particles in 3D-reconstruction) is indicated with an arrow. (b) Comparison of trypsin-treated (cyan) and native Vip3Ag4 (green) single particle-derived structures.

Table S1. Molar mass and hydrodynamic analysis of Vip3Ag4 determined by SEC-MALLS.

| Parameter | Vip3Ag4 |
|------------------------|-----------------------|
| Mn (kDa) | 338 ($\pm 0.1\%$) |
| Mw (kDa) | 336 ($\pm 0.1\%$) |
| Polydispersity (Mw/Mn) | 1.006 ($\pm 0.1\%$) |
| Rh(Q)z (nm) | 6.9 ($\pm 1.8\%$) |
| Rh(Q) (ave) (nm) | 6.8 ($\pm 0.3\%$) |

Table S2. Best-fit parameters obtained from AUC SV data analysis.

| Parameter | Interference data | | | Absorbance data | | Interference data without buffer correction | | |
|--------------------------|-------------------|-------|-------|-----------------|-------|---|-------|-------|
| Concentration (mg/mL) | 1.00 | 0.50 | 0.25 | 0.50 | 0.25 | 1.00 | 0.50 | 0.25 |
| Fit rmsd | 0.017 | 0.005 | 0.004 | 0.012 | 0.008 | 0.105 | 0.058 | 0.029 |
| sw (S) | 3.8 | 6.4 | 8.2 | 6.6 | 8.5 | 3.9 | 6.5 | 8.4 |
| sw _(20,w) (S) | 4.1 | 6.9 | 8.8 | 7.1 | 9.1 | 4.1 | 6.8 | 8.8 |
| Peak (% of total) | 99.5 | 98.0 | 54.6 | 68.3 | 67.0 | 11.0 | 6.2 | 3.8 |
| f/f ₀ | 4.0 | 2.5 | 2.0 | 2.3 | 1.9 | 3.4 | 1.8 | 1.4 |
| MW (kDa) | 301 | 326 | 352 | 311 | 335 | 236 | 200 | 197 |
| Stokes radius (nm) | 17.6 | 11.3 | 9.5 | 10.4 | 8.7 | 13.8 | 7.0 | 5.3 |
| a/b (oblate) (nm) | 65.7 | 36.4 | 17.8 | 24.9 | 14.8 | 51.7 | 12.7 | 5.1 |
| a/b (prolate) (nm) | 74.9 | 33.6 | 15.6 | 22.1 | 13.0 | 52.0 | 11.2 | 4.8 |